POLITECNICO DI TORINO
Repository ISTITUZIONALE

Washing resistant antibacterial composite coatings on cotton textiles

(Article begins on next page)

14 November 2024

Washing resistant antibacterial composite coatings on cotton textiles

Washing resistant antibacterial composite coatings on cotton textiles

Angelica Luceri [1], Sergio Perero [1], Andrea Cochis [2], Alessandro C. Scalia [2], Lia Rimondini [2], Monica Ferraris [1], Cristina Balagna [1,*]

1Department of Applied Science and Technology, Politecnico di Torino, Corso Duca degli Abruzzi 24, Turin, Italy

2 Department of Health Sciences, Center for Translational Research on Autoimmune and Allergic Diseases-CAAD, Università del Piemonte Orientale UPO, Novara, 28100, Italy

*Corresponding author:

Tel.:+39 011 0904325

Fax : +39 011 0904699

E-mail address: cristina.balagna@polito.it

Abstract

Several techniques have been developed to confer antibacterial properties to cotton textiles using silver nanoparticles (AgNPs). However, the antimicrobial performance of such a modified fabric can drastically decrease after a washing treatment. The aim of this work has been to develop antibacterial composite coatings with improved water resistance, deposited on cotton via the co-sputtering technique. The thin coatings, composed of a silica, alumina or zirconia matrix, with well embedded silver nanoclusters, were made to homogenously cover the cotton threads. The amount of silver was modulated, as was the power applied to the target, that is, 3W for a lower amount and 5W for a larger amount. The release of silver ions from the coatings into distilled water was very low, even after 14 days (less than 1 ppm) for all the coatings. The coated and uncoated cotton textiles were directly infected with the textile-colonizing pathogens *Escherichia coli* and *Pseudomonas aeruginosa*. After 24 hours, a count of the colony forming units (CFU) revealed that the textiles coated with either the silver nanocluster/silica or zirconia matrix coatings were effective in preventing the adhesion and proliferation of *E. coli* bacteria, thereby preserving the textiles from contamination. However, *P. aeruginosa* was only absent in the case of the silica coatings or when the zirconia and alumina matrix coatings contained a large amount of silver. In all the considered cases, the CFU number was reduced with respect to the uncoated textiles. The durability of all the coatings was verified after ten washing cycles. Finally, coated textiles reported to be cytocompatible towards human fibroblasts and keratinocytes after simulating the release of toxic compounds or by directly seeding cells onto materials' surface.

Keywords: silver nanoclusters; composite coating; co-sputtering; antibacterial.

Acknowledgments

2

Introduction

Nanotechnologies make textile materials "functional and smart", as they confer them with UV resistance, thermal insulation, electrical conductivity, antifouling, self-cleaning and antimicrobial properties (AkbarShah et al. 2022). The latter is a particularly "hot" topic, because textiles constitute fertile grounds for the colonization of microorganisms, due to their ability to retain moisture and dirt (Periolatto et al. 2017). In addition, the proteins contained in keratin fibres, and the carbohydrates contained in cellulose fibres are useful for the metabolism of microorganisms (Gao and Cranston 2008). Microbial contamination affects the aesthetic aspect and mechanical resistance of fibres and, more importantly, it represents a risk for users and their health, as it acts as a transport vector for potentially harmful, sometimes fatal, bacteria, fungi and viruses (Periolatto et al. 2017). For these reasons, it is particularly important to confer antimicrobial properties to textiles, considering the wide use of these materials in different application fields, from personal use to the world of sports, public transport and for the personnel working in various sectors, including health, livestock and food.

The effects of several antibacterial agents have already been studied in depth as regards the textile industry (Ibrahim et al. 2021; Windler et al. 2013). Among these agents, nanoparticles of noble metals and metal oxides have been considered as interesting biocide agents, thanks to their marked antibacterial effect on a wide spectrum of Gram-positive and Gram-negative bacteria, as well as against "superbugs", microorganisms immune to traditional antibiotics and antimicrobial agents. Silver nanoparticles are the most well-known and most exploited to date (Deshmukh et al. 2019; Souza et al. 2019; Rai et al. 2009). Their mechanism of action involves a combination of multiple processes, including the effect of released Ag ions or Ag nanoparticles (NPs) themselves, which are able to break away and penetrate the cell membrane of a bacterium, and thus modify its vital functions (Deshmukh et al. 2019; Rai et al. 2009; Pal et al. 2007).

Several methods have been developed in the textile field to produce antibacterial fabric, such as precursor doping, functionalization and surface treatments (Deshmukh et al. 2019; Radetić 2013; Granados et al. 2021). For example, silver nanoparticles (AgNPs) can be incorporated into fibres, after mixing them with precursor agents. However, this method increases the risk of a potential decrement of the antibacterial effect because the nanoparticles inside the fibre do not interact

3

directly with the external environment. On the other hand, an increase in the number of NPs to overcome this limit could decrease the mechanical and aesthetic properties of a textile. An alternative technique consists in binding nanoparticles to the material by means of a surface treatment. In this case, the goal is to increase the ability of the NPs to remain bonded to the textile surface (Radetić 2013; Granados et al. 2021). The so-called "wet methods", which are based on the use of a medium to create a suspension of in-situ or ex-situ synthetized NPs, are the most commonly used, although they suffer from the disadvantage of having a strong environmental impact, due to the use of water and chemical reagents, and of deteriorating the substrate when high temperatures are required (Kowalczyk et al. 2018; Shaban et al. 2016; Raza et al. 2015; Jain et al. 2022; Mishra and Butola 2017) .

Among "dry methods", which also include electrospray deposition (Soliwoda 2015), pulsed laser deposition (Shahzad et al. 2016; Angelina et al. 2017), arc plasma deposition (Park et al. 2016), cold spraying (Samuel et al. 2017), the sputtering technique can be used for the deposition of antibacterial coating on thermosensitive materials and defined environmental-friendly because no dangerous chemical elements and solutions are required or produced as waste (Ferraris et al. 2010).

Healthcare-associated infections are nowadays considered among the most common complications related to the hospitalization of patients; in fact, when an infection occurs, a direct increase in the number of days spent in hospital, in mortality and in the general costs unfortunately have to be expected (Allegranzi et al. 2013). In general, endogenous flora from patients is considered to be the primary source of contamination; however, the healthcare environment should also be considered to play an important role when considering exogenous infections (Weber et al. 2012). Medical instruments and high-touch surfaces (such as door handlers) are considered to be the most probable sources of contamination; however, recent literature has demonstrated that soft surfaces and healthcare textiles can also easily be infected by pathogens, and thus rapidly become a primary source of the spread of infection (Heudorf et al. 2017). In fact, it has been demonstrated that such strains as *Escherichia coli*, *Pseudomonas aeruginosa, Staphylococcus aureus* and *Enterococcus faecium* can survive for up to 20-21 days on cotton or polyester textiles after adhesion (Riley et al. 2017;

4

Fijan et al. 2017). Professional laundry procedures, involving a high temperature application (70-90°C, for 10-20 minutes), are normally applied to ensure a complete decontamination of healthcare textiles. However, it is known that some countries (such as the United Kingdom) allow professional healthcare textiles to undergo domestic laundering as well as the use of low temperature treatments (60°C, for 10 minutes), thus opening the way toward a non-complete eradication of bacteria (Owen and Laird 2020). Moreover, domestic laundry procedures obviously do not undergo any professional test to validate the complete eradication of bacteria, which instead is commonly applied after industrial laundering. Therefore, the introduction of surface modifications to intrinsically make textiles highly antibacterial could be an interesting strategy to prevent, or at least to reduce, the healthcare contamination risk due to infected textiles. This goal can be achieved by introducing an agent that is able to kill bacteria through direct contact, for example, by using silver, as in Liu et al. (2021), or by preventing the adhesion of early-colonizing bacteria, as reported by Sharifikolouei et al. (2021), which involves exploiting superhydrophobic surfaces.

Ferraris et al. (2010, 2019) patented and developed a composite antimicrobial/antiviral coating constituted by silver nanoclusters that were well embedded in a glass or ceramic matrix, and in particular in a silica matrix (Ferraris 2010, 2019). The coating, obtained via the co-sputtering technique, showed excellent adherence to the substrate, good resistance at high temperatures, good flexibility and excellent antimicrobial/antiviral properties (Ferraris et al. 2010; Irfan et al. 2017; Balagna et al. 2020b; 2021). As reported by Irfan et al. (2017), this co-sputtered coating has already been used for the functionalization of cotton to make it have the same characteristics as healthcare textiles. Exploiting such a preventive activity is possible thanks to the well-known antibacterial properties of silver, which have largely been demonstrated to be able to kill bacteria through direct contact (irreversible formation of membrane pores) or to stop their replication (through direct DNA denaturation) (Bruna et al. 2021). However, using silica as a matrix results in a high solubility in water, which makes the coating unsuitable for prolonged contact with aqueous solutions. Since textiles are capable of retaining moisture and may be subjected to several washings, alternative matrices have been investigated in this work.

5

Therefore, the aim of the present work has been to deposit and characterize silver nanocluster doped/ceramic matrix composite coatings, which had been designed to show high resistance to water solutions, on cotton textiles. Zirconia and alumina were selected as the matrices, and the obtained results were compared with those of previously studied silica matrix composite coatings (Irfan et al. 2017). Morphological and chemical analyses were conducted. Ion release tests were conducted to measure the amount of silver ions released into the water solutions.

Specimens were infected with *Escherichia coli* and *Pseudomonas aeruginosa*, two of the main pathogens involved in textile colonization (Owen and Laird 2020), in order to verify their ability to prevent the adhesion and spread of the bacteria on the tested textiles. The stability to washing was verified through EDS analysis and antibacterial tests conducted on coated samples after several washing cycles. Finally, to exclude any toxic side effect due to the coatings, the cytocompatibility of coated cotton was verified by both indirect and direct assays towards human fibroblasts and keratinocytes, cells representative for dermis and epidermidis.

Materials and methods

Sample preparation

The radio-frequency co-sputtering technique was utilized to deposit silver nanocluster/silica, or ceramic matrix composite coatings, onto cotton used as a substrate, according to a patented method, with Kenosistec[TM] equipment (Ferraris et al. 2010a, 2019). The cotton is a woven fabric dyed green (290 g/m^2) with warp and weft yarn count 24/1 Ne (supplied by Iniziative Industriali Sas Italy). The thin composite coating was co-sputtered using silica (99.99% SiO_2, Nanovision [TM]), alumina (99,98% Al_2O_3, Franco Corradi [TM]) or zirconia (99,98% ZrO_2, Nanovision [TM]) targets to obtain a matrix, and a pure silver target (99.99% Ag, 5Pascal [TM]) to obtain nanoclusters. The deposition procedure lasted 1hour, and was conducted, under a controlled Ar atmosphere, by applying different levels of power to the targets: 200, 250 and 290W for silica, alumina and zirconia, respectively, and 3, 5 and 10 W to the silver target. The coatings will be called "Cotton" for uncoated textile and "SiO2-Ag3/SiO2-Ag5" or "Al2O3-Ag3/Al2O3-

6

Ag5" or "ZrO2-Ag3/ ZrO2-Ag5" as acronyms for cotton coated by the different coatings.

Morphological, compositional and structural analyses

Energy Dispersive X-ray Spectrometry (EDS, PV 990^{TM}) was used to determine the elemental composition of the substrates and of the coatings, in terms of at. % of Ag, and of the metal constituting the oxide of the matrix (Si, Al or Zr). Three areas of each sample were analyzed at a low magnification (150x) for the statistical analysis, and the results were then used for a preliminary selection of the deposition parameters and to compare the results with those obtained in previous papers (Balagna et al. 2017, 2019, 2020a, 2021). An important parameter that needs to be considered is the ratio between the % atomic amount of Ag and that of the metal (M) constituting the matrix:

$$\frac{\%at.\,Ag}{\%at.\,Ag + \%at.\,M}$$

Samples are considered suitable for the followed analysis when they have a ratio of between 0.3 and 0.5, as mentioned in previous paper (Irfan et al. 2017). A low ratio corresponds to non-effective antibacterial behavior, while a high ratio could lead to the formation of larger silver clusters than the nanoscale.

A more in-depth compositional analysis was performed, through X-Ray Photoelectron Spectroscopy (XPS, Phi 5000 Versa Probe™), to evaluate the elements that constituted the first atomic layers and their bond state. A monochromatic Al Kα X-ray source was used for this analysis, with photon energy of 1486.6 eV at 15 kV and 1 mA. In order to calibrate the binding energy scale, the carbon C1s (C-C) binding energy was set at 284.5 eV. This test was conducted on uncoated and coated cotton.

 An X-ray diffractometry (XRD, Bragg-Brentano X'pert Philips diffractometer) analysis was conducted to determine the presence of an amorphous or a crystalline matrix, in addition to the presence of nanoclusters. The analysis was performed in X-ray grazing mode, with a low constant angle of 1°, but only to evaluate the coated sample surface, which had been deposited on a soda-lime glass substrate.

A UV-Visible adsorption analysis (Uv-Vis, Shimadzu, UV 2600) was conducted, over the 200 nm and 700 nm range, to investigate the presence of silver

7

nanoclusters. The analysis was performed on soda-lime glass substrates that had only been coated with the matrix and on substrates with silver nanocluster/ matrix composite coatings, which were used for comparison purposes.

The morphology of the coatings was observed by means of a Field Emission Scanning Electron Microscope, (FESEM, Quanta Inspect 200, Zeiss Supra 40[TM]). The surface of the samples was observed under different magnifications also in back scattered mode, in order to confirm the deposition of the coating and the formation of nanoclusters, as well as to evaluate their dimension and dispersion in the matrix. A comparison was made with the uncoated cotton.

The coating thickness was detected, in triplicate, by means of a contact profilometer, (Taylor & Hobson, Intra), on coatings deposited onto silicon substrates. The coatings were only deposited onto half of each silicon substrate, and the other half was covered with an adhesive tape to obtain a step on the substrate and to measure the different heights of the two areas.

Silver amount and leaching test

The amount of silver present in the samples SiO2-Ag5, Al2O3-Ag5 and ZrO2-Ag5 was determined by Inductively Coupled Plasma Mass Spectroscopy (ICP–MS, Thermo Scientific iCAP™ Q ICP–MS). Samples of 1x1 cm^2 (about 0,015g) were immersed in 5 ml of nitric acid and heated for 30 minutes. Then distilled water was added to the solution till a final volume of 25 ml was reached. In order to evaluate the concentration of silver released in water, coated samples ~~Sample~~ (1x1 cm^2) were immersed in 30 ml of milliQ water at room temperature, with the coated surface facing upward. The solution was analyzed after 1 hour, 3 hours, 1 day, 7 days and 14 days, using a Hanna Instruments[TM] spectrophotometer, to measure the concentration of silver ions (ppm) released into the water. The test was repeated on three samples for each time.

Antibacterial evaluation

The used *Escherichia coli* (EC, ATCC BAA-1161) and *Pseudomonas aeruginosa* (PA, ATCC 15442) pathogenic biofilm-former certified strains were both obtained from the American Type Culture Collection (ATCC, Manassas, USA) and cultivated according to the manufacturer's instructions. Accordingly, EC was

8

cultivated on Luria Bertani agar plates (LB, from Sigma), whereas PA was cultivated on trypticase soy agar plates (TSA, from Sigma) for 24 hours at 37°C till single round colonies were observed; the day after, 2 colonies from each plate were collected and resuspended in a fresh broth culture for 2 hours under agitation (90 rpm) in order to achieve the logarithmic growth phase. Finally, the broth culture was diluted with a fresh medium until the optical density was 0.001 at a 600 nm wavelength, thus corresponding to 1×10^5 bacteria/ml (Rivera et al. 2021). Specimens were submerged in 1 ml of the above-mentioned bacterial suspension to obtain a direct infection of the control and test textiles; after 24 hours of cultivation at 37°C, the specimens were collected and placed in 15 ml tubes containing PBS, and the surface-colonizing bacteria were mechanically detached from the specimens by means of sonication and vortexing (3 times each, for 30 seconds). The number of viable bacteria was determined by means of a colony forming unit (CFU) count, as previously detailed by the authors (Cochis et al. 2021), according to the following formula:

$$CFU = (number\ of\ colonies \times dilution\ factor)^{(serial\ dilution)}$$

The antibacterial assays were performed in triplicate. The obtained data were analyzed using SPSS software (v.20.0, IBM, USA). After confirming the distribution and homogeneity of variance, by means of the Shapiro-Wilk and the Levene tests, the groups were compared, by means of one-way ANOVA, using the Tukey test for the post-hoc analysis. Significant differences were established at $p < 0.05$.

Resistance to washing

The coated cotton textiles were washed to evaluate the resistance of the different coatings to repeating washings. Three coated samples were immersed in a solution of 100 ml of milliQ water and 0.2 g of detergent (1993 WOB Standard detergent without any optical brightener, and without phosphate, Testfabrics, Inc.). The test was performed in a thermostatic bath at 50°C for 30 minutes, at an oscillation rate of 130 rpm, on smaller samples (20 mm x 20 mm) than those generally used in washing machines, to simulate a washing machine process in the lab. The samples were then rinsed with distilled water to remove any detergent residuals. Different washing cycles (1, 5 and 10) were performed on each sample, and the amounts of

9

silver and of the matrix were evaluated through an EDS analysis. In addition, the samples were tested, by means of an inhibition halo test using *S. epidermis* strain (Standard NCCLS 2003), in order to evaluate the antibacterial effect after 10 washing cycles. The sample was also analyzed before being washed for comparison purposes.

Cytocompatibility evaluation

The uncoated and coated cotton samples were evaluated for their *in vitro* cytocompatibility by both direct and indirect assays toward human fibroblasts (HGF, PCS-999-04 from the American Type Culture Collection - ATCC) and human keratinocytes (HACAT, from Lonza). Cells were cultivated following Manufacturers' instructions till 90% confluence, detached by trypsin-EDTA and used for experiments: accordingly, HGF were cultivated in alpha-modified Eagle Medium (a-MEM from Sigma-Merck) supplemented with 10% foetal bovine serum and 1% antibiotics (penicillin/streptomycin), while HACAT were cultivated in RPMI (from Sigma-Merck) supplemented with 10% foetal bovine serum and 1% antibiotics, both at 37°C, 5% CO2.

The indirect evaluation was performed according the guidelines reported in ISO 10993-5 "Tests for in vitro cytotoxicity". Briefly, specimens (1x1 cm^2 side squares) were submerged in 10 ml of medium for 7 days at 37°C in agitation (120 rpm in an orbital shaker) in order to force them releasing any potentially toxic elements. Afterwards, supernatants were collected and used to cultivated cells seeded in a defined number into 24 multiwell plates (2x10^4 cells/well, 1 ml of pre-conditioned medium/well). After 24 hours incubation at 37°C, the metabolic activity of the cells was evaluated by the colorimetric metabolic assay alamar blue (AlamarBlue™, ready to use solution, from Thermo Fisher) by reading fluorescence by spectrophotometer (Spark, Tecan). Cells cultivated with fresh medium were considered as control and the results were expressed as relative fluorescent units (RFU) and normalized to the control that was assumed to be 100% viability. To further investigate cells' density and morphology, cells were stained with the fluorescent dyes phalloidin (from Thermo Fisher) and 4′,6-diamidino-2-phenylindole (DAPI, from Thermo Fisher) to co-visualize cytoskeleton f-actins filaments and nuclei, respectively, after 24 hours in direct

10

contact with pre-conditioned medium. Images were collected with a confocal microscope (Leica TCS SP8 LIGHTNING confocal laser scanning microscope).

For the direct assay, cells were seeded directly onto the surface of samples in a defined number ($2x10^4$ cells/specimen) and cultivated for 48 hours at 37°C; then, the metabolic activity of the cells was evaluated by the metabolic assay almar blue as previously detailed whereas the morphology was visually checked by scanning electron microscopy (SEM, JEOL JSMIT500) after dehydrating specimens by the alcohol scale (70-90-100% ethanol, 20 minutes each, room temperature), fixing them onto stubs with conductive carbon and gold surface metallization.

Direct and indirect assays were performed in triplicate. The obtained data were analyzed using SPSS software (v.20.0, IBM, USA). After confirming the distribution and homogeneity of variance, by means of the Shapiro-Wilk and the Levene tests, the groups were compared, by means of one-way ANOVA, using the Tukey test for the post-hoc analysis. Significant differences were established at $p < 0.05$.

Results and discussion

Morphological, compositional and structural characterization

When the elemental composition of both the coatings and the substrate was analyzed, the EDS analysis verified the presence of the coatings on the cotton surface. The analysis of the cotton only detected oxygen, carbon and traces of Ca. After the coating deposition, the presence of silver and silicon, aluminium or zirconium, was detected on the surface of the samples. An application of the power applied to the matrix targets of 200W was selected for SiO_2, while 290 W was selected for Al_2O_3 and ZrO_2, and it was varied from 3 to 5 W for Ag. Table1 reports the atomic percentages of the metallic elements of the matrices (Si, Al or Zr, indicated as M) and the Ag of the selected coatings.

The atomic percentage amount of Ag increased as the power applied to the target was increased, passing from 3 W to 5 W, whereas the values of the %at. of Si, Al or Zr remained almost unchanged for both depositions. This caused an increment in the value of the Ag/M+Ag ratio between the two depositions for each matrix. In the case of the deposition with 3 W of power on the Ag target, this ratio varied between 0.3 and 0.5. In the case of 5 W of applied power, the ratio remained

11

constant at 0.5, thus demonstrating good reproducibility of the process, even in the case of different matrices.

The XPS analysis confirmed the composition of the coatings. Fig. 1 reports the XPS spectra of the three coatings containing silver, albeit only at 3W, and compares the results with the uncoated cotton graph. The uncoated cotton showed C1s peaks at 284eV and O1 peaks at 532 eV, because it is only composed of cellulose (Irfan et al. 2017). After the deposition, peaks appear on the silica-based coating, that is, Si2p at 102 eV, and Si2s at 150 eV, on the alumina-based coating, Al2p at 71 eV, and Al2s at 117 eV, and on the zirconia-based coating, Zr-4s at 29 eV, Zr-3d5 at 180 eV, Zr-3p3 at 330 eV and Zr-3p1 at 344 eV. Moreover, peaks related to metallic silver were detected on all the coatings, in particular Ag-3d3 and d5 at 370, 367 eV and Ag-3p1 e p2 at 602, and 570 eV.
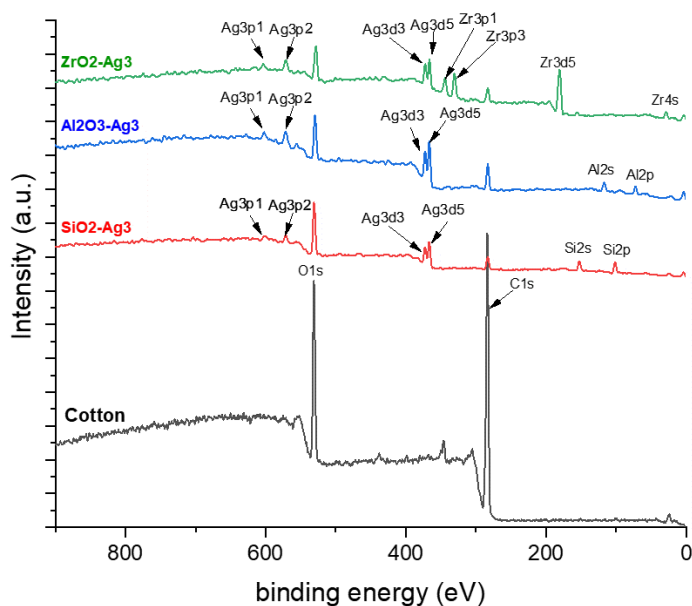

Fig. 1 XPS survey spectra of the (a) uncoated cotton, (b) silica-based coating (SiO2-Ag3), (c) alumina-based coating (Al2O3-Ag3), and (d) zirconia-based coating (ZrO2-Ag3).

The data relative to the composition of the coatings (only Ag 3W) and to the cotton, in terms of % at. obtained from the XPS analysis, are summarized in Table 2, where C and O are confirmed as the main elements of the uncoated substrate. After deposition of the coating, the at.% of C decreased, whereas the amount of O increased, due to the deposition of the matrix oxides. The quantities of Si, Al, Zr and Ag resulted to be somewhat similar for all the coatings.

12

Fig. 2 reports the graphs related to the high-resolution spectra of the individual peaks of the C, O, matrix metal, and Ag of the three coatings and compares the curves with those of cotton (only C and O). The C1s spectrum of the uncoated cotton in Fig. 2a was deconvoluted into 3 subpeaks, according to the different bondings. The peak at 284.9 eV was assigned to C–C and C–H bonds the peak at 286.3 eV to C–O, and the peak at 288 eV to the C=O and O–C–O bonds (Jazbec et al. 2015). C-O, C-O-C and O-C-O are particular bondings of cellulose, while the C-C and C-H bondings are probably due to impurities or additives (Irfan 2017).

The spectra of the C1s changed after the deposition of the coating. Only the peak relative to C-C and C-H remained clearly visible at around 284.9 eV for the three coatings, whereas a broad peak at 288 eV was only detected in the SiO2-Ag3 sample, with the substrate contributing less to the C-1s spectra in the first nanometres of the composite coating.

The graph in Fig. 2b is related to the O1s. The peak at 532,62 eV in the cotton curve is associated with C-OH and C-O-C bondings, which are typical of cellulose (Irfan et al. 2017; Jazbec et al. 2015). The peaks at 532,69 eV, 531,2 eV and 529,7 eV in the spectra, relative to the coatings, are associated with the bonds between O and the metal forming in the matrix, that is, Si-O, Al-O and Zr-O, respectively. In the case of zirconia coating, the O1s peak can be split into two peaks, Zr-OH and Zr-O (Stefanov et al. 2000; Gottardi et al. 2008).

The graph in Fig. 2c is divided into three, according to the three different x-axes used to analyze the coating matrices. The coatings with silica and the alumina matrix both show the presence of only one peak at 103,34 eV for SiO2_Ag3, and at 74,94 eV for Al2O3_Ag3, associated with the Si-O and Al-O groups, respectively. Two split peaks, related to Zr3d at 184 and 181,64 eV can be attributed to the oxide ZrO_2.

Lastly, Fig. 2d shows the spectra related to silver. Two peaks, at 374 and 368 eV, can be attributed to Ag3d-3/2 and Ag3d-5/2, thus indicating Ag^0 and confirming the presence of nanoclusters of metallic Ag on all three coatings (Rehan et al. 2015; Volkov et al. 2017).
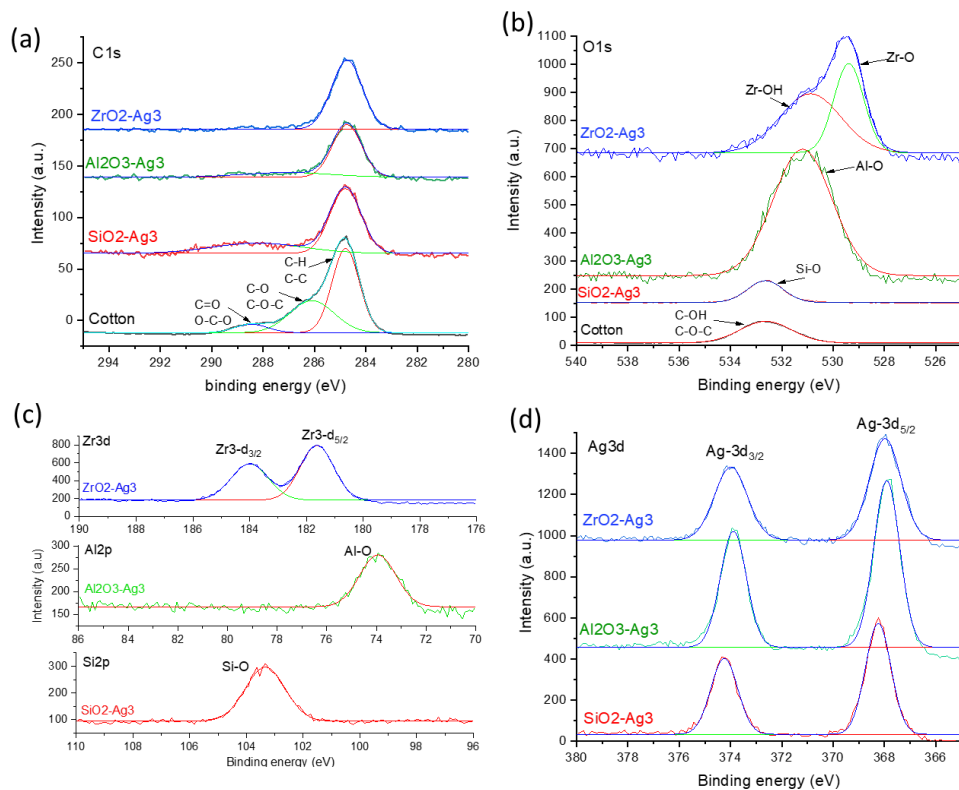
13

Fig. 2 High resolution XPS spectra of carbon, oxygen, the metals of the matrix oxides (Si, Al and Zr) and silver: comparison among the cotton coated with the three coatings of silica or alumina or zirconia and silver nanoclusters (3W) and the uncoated cotton.

Fig. 3 reports the XRD spectra relative to the three coatings with large (Ag5) and small (Ag3) amounts of silver, and compares the results with the sample coated only with the related matrix of silica, alumina or zirconia. The spectra of the SiO2-Ag and Al2O3-Ag coatings (Fig.3a and b) are very similar to the spectra pertaining to the presence of silver on the composite coatings, that is, they show the presence of the amorphous halo of the matrix at 2θ between 15 and 35°, and the peaks at 2θ=38°, 44°, 64°, 77°, 81°. XRD analysis confirmed the metallic state of silver nanoclusters because of the correspondence of the detected peaks with those of the reference pattern relative to metallic Ag (ref code PCPDF 01-089-3722). The intensity of the silver peaks increases for a larger amount of silver, as obtained with power on the target at 5W. Moreover, the amorphization of the alumina is typical of the deposition of a thin film by means of the PVD technique, such as the sputtering process, even though the target is made up of crystalline alumina (Zuzjaková et al. 2013).

14

In a different way, the zirconia matrix (ZrO2 in Fig. 3c) remained crystalline, even after the sputtering process, as confirmed by the presence of the peaks in the spectra. The deposition of the two composite coatings tended to induce amorphization of the matrix with an enlargement of the peaks, especially at 2θ between 20 and 30° of ZrO2-Ag5 coating. The ZrO2-Ag3 coating have low peaks relative to silver due to the lower amount of the element, detected by EDS analysis, compared with ZrO2-Ag5 coating.

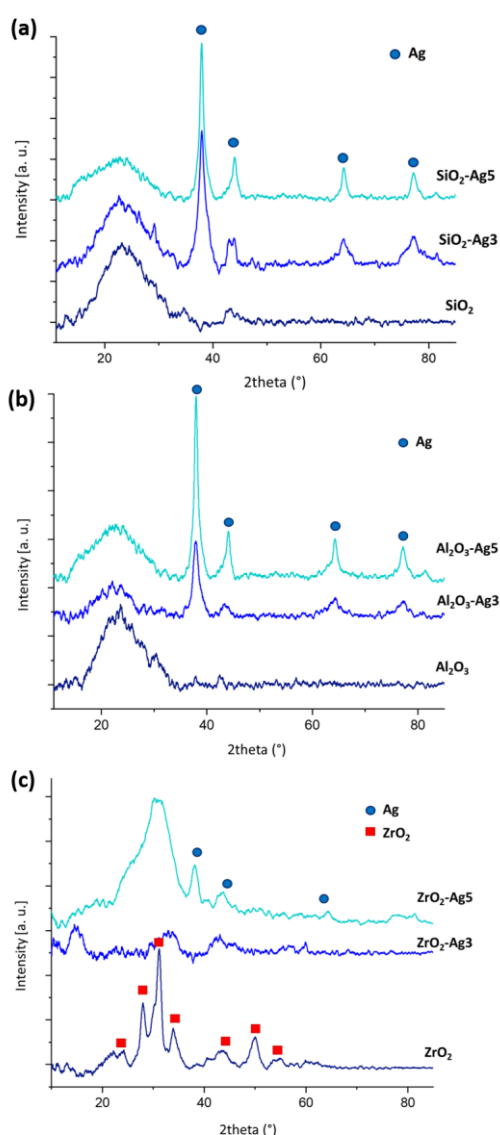**Fig. 3** XRD analysis of the coatings (a) SiO2-Ag, (b) Al2O3-Ag, and (c) ZrO2-Ag with the two different silver concentrations (Ag5, high amount, and Ag3, low amount), and comparison of the spectra with those obtained for the corresponding matrix (silica, alumina or zirconia, respectively). *(Samples deposited on soda-lime substrates)*

15

The UV-Visible spectra obtained from the matrices and nanostructured composite coatings are reported in Fig. 4. None of the matrices show any absorption peaks. The spectra relative to the composite coatings, based on silica and the alumina matrix (Fig. 4a, b), show a clearly visible peak at 414 nm, due to the plasmonic resonance of silver nanoclusters, as was also reported in a previous paper (Ferraris et al. 2010b). This peak is higher and shifted to a wavelength of 427 nm in the case of SiO2-Ag5, probably due to a slight increment in the size of the nanoclusters or an increment of the Ag amount (Krilova et al. 2009). The spectra of the zirconia composite coatings (Fig. 4c) are somewhat different. The peaks are in the 448-466 nm and 376-385 nm ranges for Ag3 and Ag5, respectively, and they can be attributed to the plasmonic resonance of silver nanoclusters. As in the case of the silica matrix, when comparing the two spectra containing silver, the peak in the ZrO2-Ag3 curve appears to be shifted to a higher wavelength, widened and less intense, probably due to a smaller quantity of silver (Krilova et al. 2009).
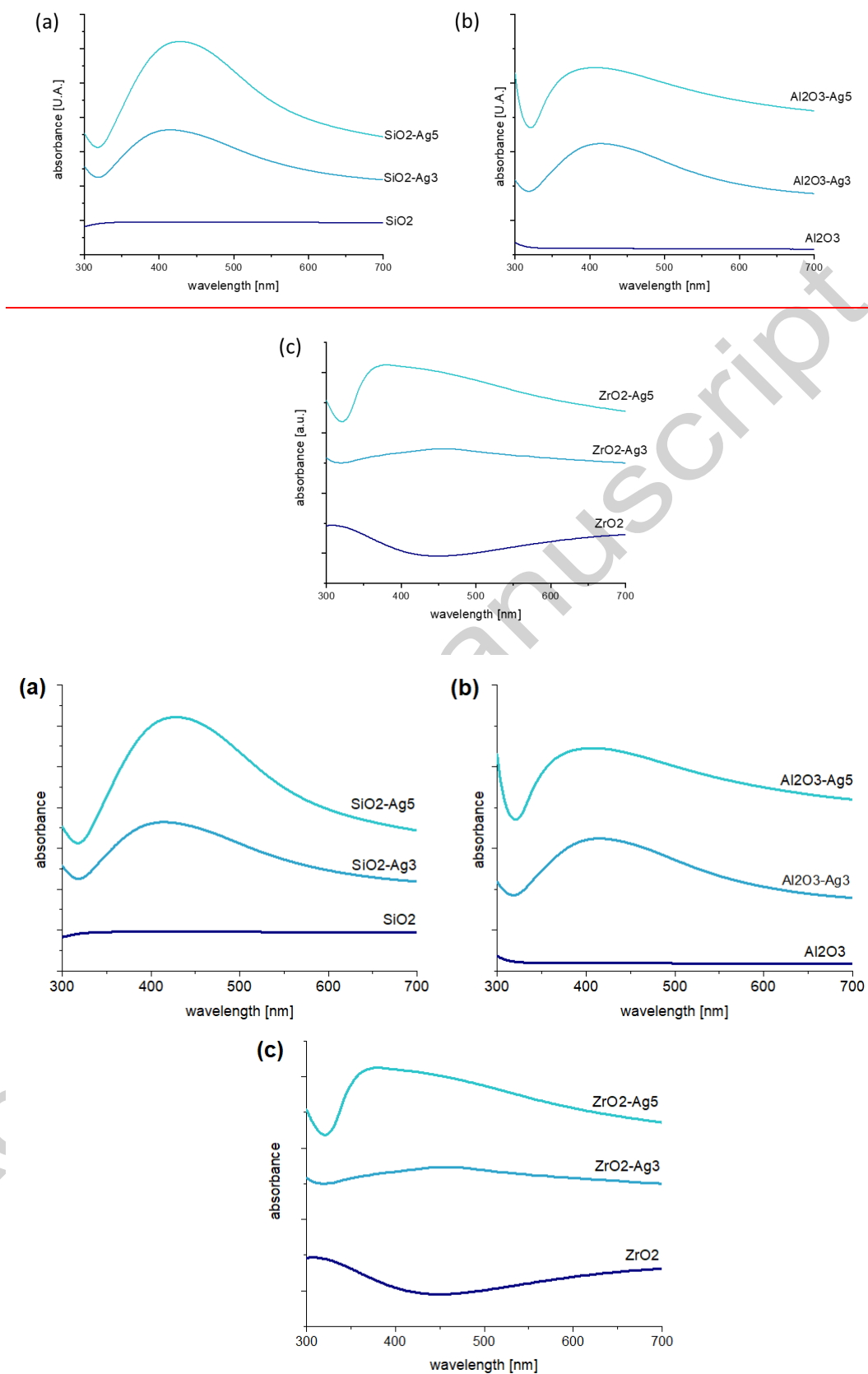
16

Fig. 4 Uv-Visible analysis of the (a) SiO2-Ag, (b) Al2O3-Ag, and (c) ZrO2-Ag coatings *(Samples deposited on soda-lime substrates)*

17

17

Fig. 5 and 6 report FESEM images of the uncoated and coated cotton, in secondary electrons and back scattered mode, respectively. ~~Cellulose fibrils are clearly visible on the uncoated fibre~~ The characteristic surface of cotton fibre is visible (Fig. 5a). After the deposition, all the coated substrates (b-c for SiO2-Ag, d-e for Al2O3-Ag and f-g for ZrO2-Ag) are characterized by the same nanostructured morphology as the composite layers, and by a porous and globular-shaped matrix which uniformly covers the fibres. This kind of morphology is typical of sputtering methods, and was also observed in previous papers by the authors (Irfan et al. 2017; Balagna et al. 2017, 2019). Silver nanoclusters are not clearly visible, except for some bright particles that could be ascribed to such nanoclusters, and which are indicated with red arrows in the figure. ~~The nanoclusters are well dispersed in the matrix and difficult to observe under the microscope.~~
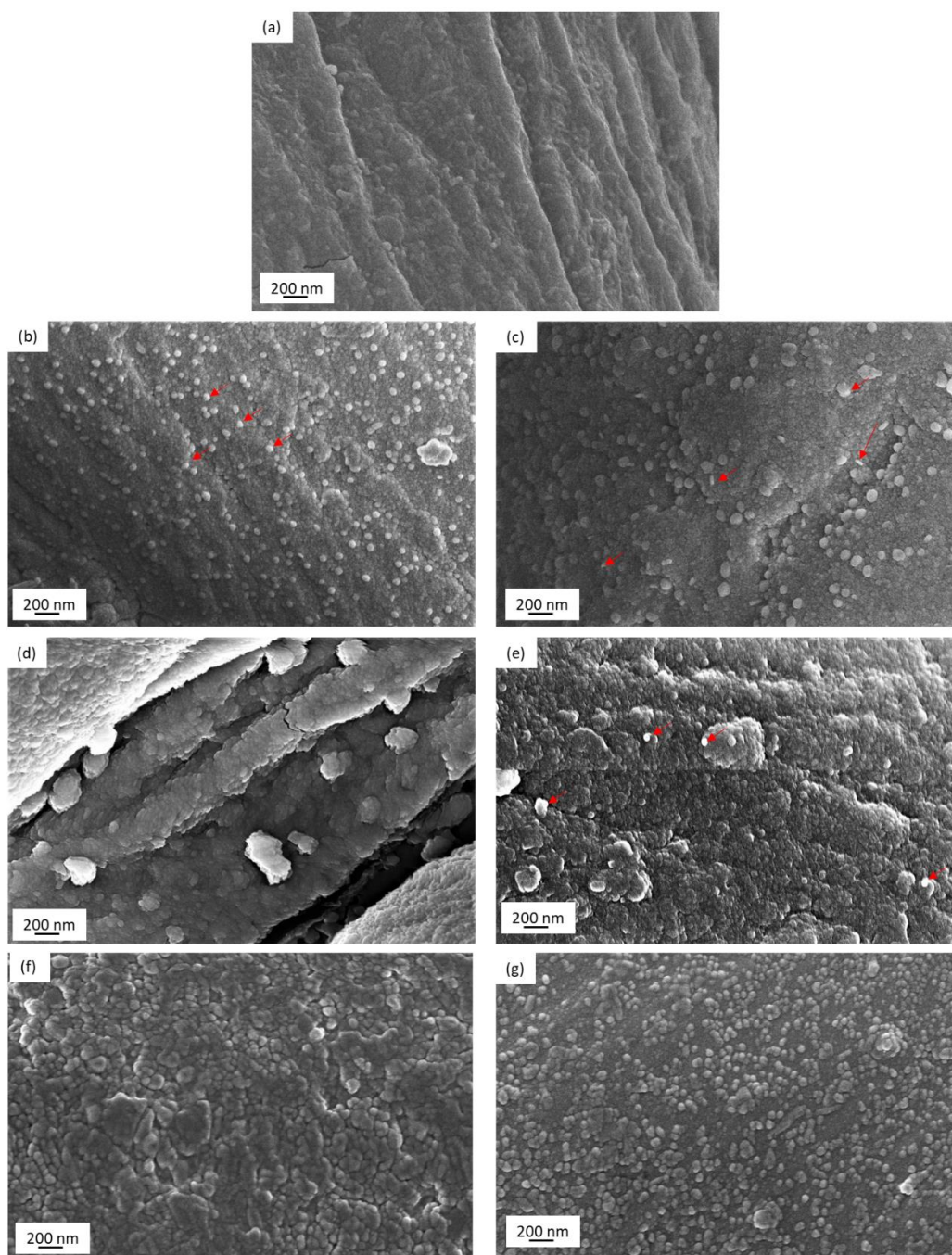
18

Fig. 5 FESEM images of the (a) uncoated cotton and cotton with coatings, (b) SiO2-Ag3, (c) SiO2-Ag5, (d) Al2O3-Ag3, (e) Al2O3-Ag5, (f) ZrO2-Ag3, and (g) ZrO2-Ag5. The red arrows indicate the presence of Ag nanoclusters on the coating surface.

The images reported in the back scattered mode relative to the coatings with higher amount of silver (Fig. 6) show the nanoclusters as distributed on the coating surfaces. They are clearly visible and more homogeneously distributed on the SiO2-Ag5 coating (Fig. 6a) even if it is possible to observe them also in the

19

other two coatings. Red arrows indicated some nanoclusters as an example in the figure.

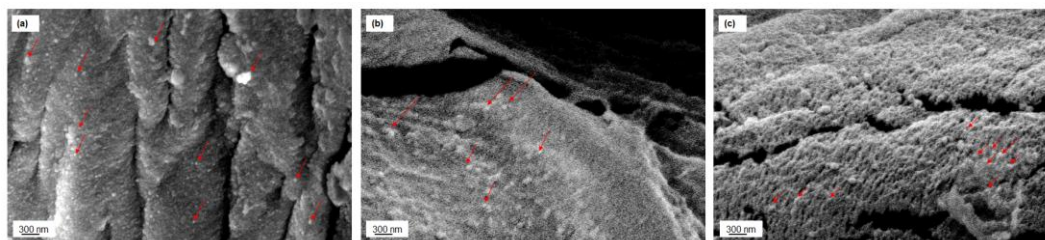**Fig. 6** FESEM images in back scattered mode of cotton with coatings, (a) SiO2-Ag5, (b) Al2O3-Ag5 and (c) ZrO2-Ag5. The red arrows indicate the presence of Ag nanoclusters on the coating surface.

The thickness of the coatings with Ag deposited at 3W was measured using a profilometer, and the following values were obtained: 69 ± 2 nm for silica, 93 ± 22 nm for alumina, and 89 ± 7 nm for the zirconia matrix.

Leaching test

The analysis through ICP-MS allowed to detect the amount of silver contained in the SiO2-Ag5, ZrO2-Ag5 and Al2O3-Ag5 coatings deposited on cotton fabrics with dimensions of 1x1 cm^2 and to compare this value with that obtained by silver ions release test. The amount of silver coating was 1.09 ± 0.02 ppm in silica matrix, 1.14 ± 0.02 ppm in the alumina matrix coating and 0.61 ± 0.02 ppm in the zirconia matrix coating.

Silver nanoparticles usually release silver ions, if they are in contact with water or an aqueous solution (Tomšič et al. 2008). Since the antibacterial effect of silver nanoparticles may depend on the released ions, a silver ion release test was performed on the coated textiles. The curves in Fig. 6 7 show the ~~number~~ concentration of silver ions released by the coatings and compares the effect of the three different matrices and the different amounts of silver (Ag3 and Ag5), evaluated after several immersion times. In general, a higher ~~number~~ concentration of ions in a solution is associated with a coating with a higher number of silver nanoclusters (Ag5), but also with a matrix with higher solubility when in contact with water. SiO2-Ag5 released the highest ~~number~~ amount of ions, and a greater release rate was observed in the first days. This release slowed down between day 3 and day 7 and reached a plateau after 14 days, where a maximum value of 0.6 ppm was observed. In the case of SiO2-Ag3, the maximum

20

value was 0.3 ppm. The ~~numbers~~ concentration of ions released by both of the silver nanocluster/alumina matrix composite coatings were comparable after 14 days. Although the number of silver nanoclusters inside the matrix was different for Al2O3-Ag3 and Al2O3-Ag5, the release trend was quite similar. Both of the silver nanocluster/zirconia matrix coating curves showed a similar trend, except for the first 3 hours of immersion, where a higher released ion rate was registered for the ZrO2-Ag5 sample. The reported values remain within the range between the minimum concentration required for antimicrobial action (0.1 ppb) and the maximum concentration considered to be toxic for humans (10 ppm) (Jamuna-Thevi et al. 2011). However, it is difficult to obtain a precise value of silver toxicity, because the effect of silver depends to a great extent on the exposition time and the area of human contact. For example, silver is not able to easily penetrate intact skin. However, the skin barrier is compromised when there is a wound on the skin or mucous. Argyria, the most-known human disease related to silver exposure and absorption, can occur for cumulative doses of silver ions and nanoparticles in the 70–1500 mg silver/kg body weight range (Hadrup et al. 2018). This range corresponds to 70-1500 ppm, which is very high compared to the results reported here.
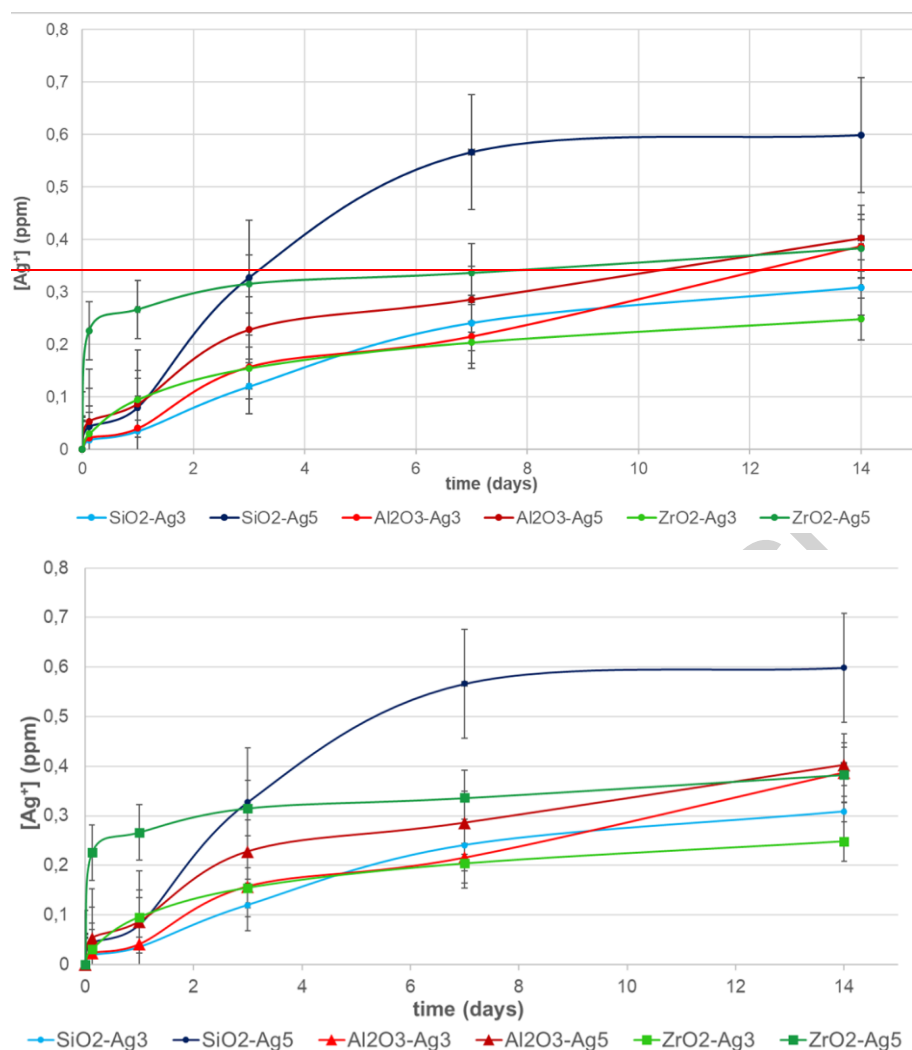
21

Fig. 6 7 Ions released from the silica, alumina and zirconia-based coatings with Ag at 3W and 5W *versus* time.

As the tested sample via ICP-MS and leaching test had the same dimensions 1x 1cm^2, it is possible to compare the initial amount of silver in each coating and the values of Ag+ released after 14 days of immersion. About 55% of the silver was released from coating with silica matrix, 35% from coating with alumina matrix and 62% from coating with zirconia matrix.

Evaluation of the antibacterial properties

Uncoated and coated cotton textiles were directly infected for 24 hours with *Escherichia coli* and *Pseudomonas aeruginosa*, two of the most important pathogens responsible for textile contamination. At the end of the selected period of time, the degree of contamination of all the tested samples was evaluated by counting the viable colonies colonizing the surface using the CFU method. The obtained results are reported in Fig. 7 8.
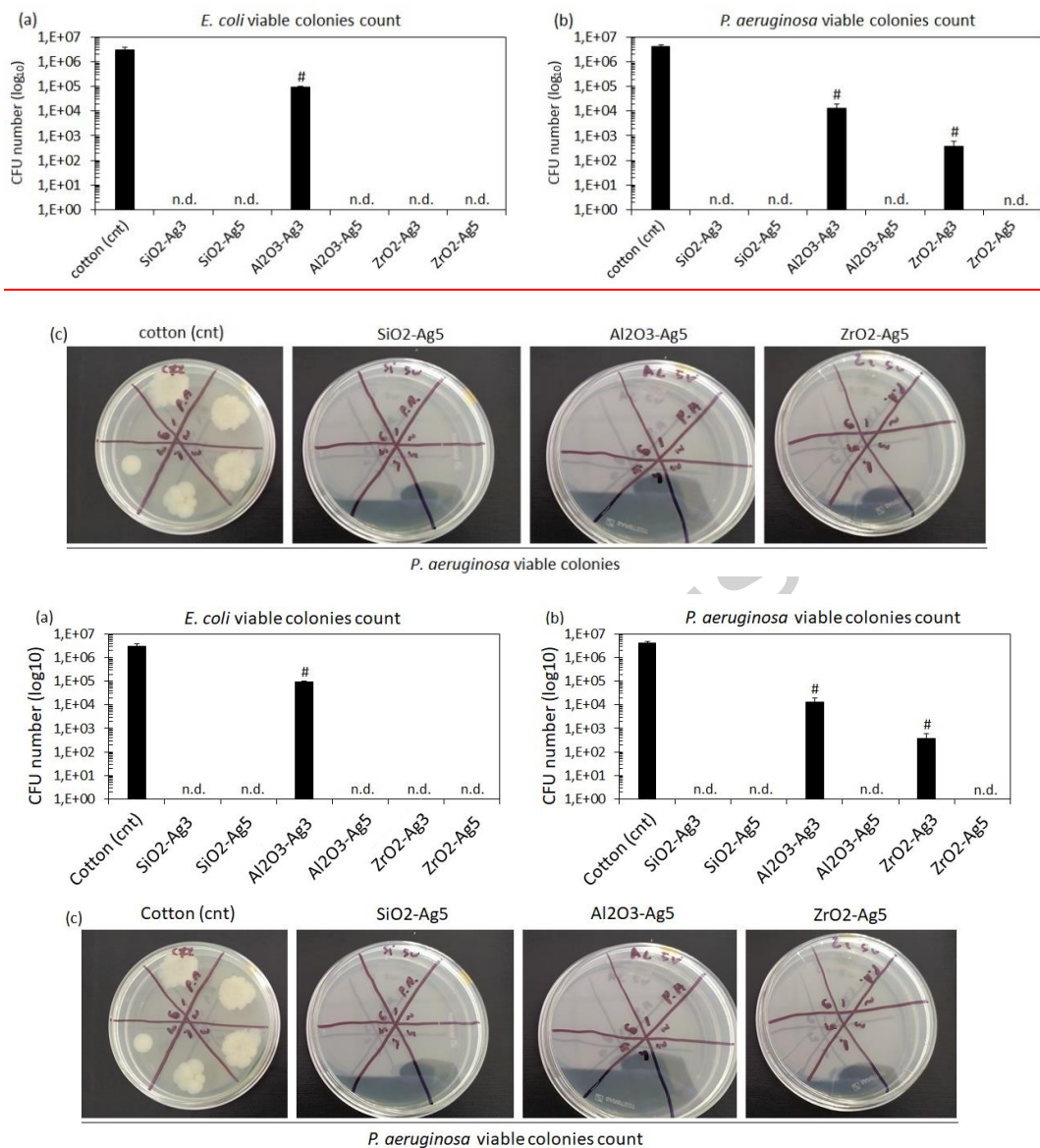
22

Fig. ~~7~~ 8 Antibacterial evaluation: histograms of the number of viable CFUs of (a) *E. coli* and (b) *P. aeruginosa* contaminating the three composite coatings with the low and the high Ag contents. Uncoated cotton was used as a control (n.d. = colonies not detected; # = p<0.05). (c) representative pictures of the living *P. aeruginosa* colonies after detachment from the composite coatings containing a large amount of silver (Ag5).

In general, the starting hypothesis of composite coatings used to confer intrinsic antibacterial properties seems to be confirmed for both *E. coli* (Fig. ~~7~~ 8a) and *P. aeruginosa* (Fig. ~~7~~ 8b). A significant reduction in CFU (p<0.05 indicated by #), compared to the uncoated cotton (cnt), was observed after 24 hours of infection. The number of viable bacteria on the uncoated cotton had increased by about 1.5 logs, compared to the starting number of CFU (1×10^5 bacteria/specimen), thus

23

confirming the ability of the tested strains to adhere and proliferate on the surface of the specimens without an antibacterial element. When considering all the cotton textiles coated with the composite coatings containing large amounts of Ag (SiO2-Ag5, Al2O3-Ag5 and ZrO2-Ag5), no viable bacteria were detected for either of the tested strains (Fig. 7 8a-b, n.d. = not detected) after 24 hours of direct infection. Representative images of the *P. aeruginosa* detached colonies are illustrated in Fig. 7 8c, which, on one hand, shows the lack of viable colonies adhering to the surface of the silver nanoclusters/composite coatings containing a large amount of silver (Ag5) but, on the other hand, a large number of grown colonies after detachment for the controls (cotton cnt).

When looking at the cotton textile coated with the lower amount of Ag in the composite coatings (SiO2-Ag3, Al2O3-Ag3 and ZrO2-Ag3), it emerges that only the coating with the silica matrix (SiO2-Ag3) was effective in preventing infection of the textiles by both strains; the composite coating with the zirconia matrix (ZrO2-Ag3) instead stopped the infection of *E. coli,* but not that of *P. aeruginosa,* which was reduced by about 2 logs ($1x10^3$ viable colonies). The coatings with the alumina matrix showed the least activity, as they indicated a bacteriostatic activity toward *E. coli* (which remained at $1x10^5$ colonies/specimen) and reduced the *P. aeruginosa* colonies by about 2 logs ($1x10^3$ viable colonies). However, the lower effect observed for the *P. aeruginosa* strain in comparison to *E. coli* can be ascribed to the known ability of the first to produce pyocyanin, a redox-active compound that can oxidize and reduce other molecules (Jayaseelan et al. 2014; Muller and Meret 2014). Muller and Merrett (2014) previously demonstrated that *P. aeruginosa* can exploit pyocyanin to reduce the amount of the bioavailable antibacterial Ag+ into the elemental nanoparticulate Ag0, which is non-toxic for bacteria. So, as a further improvement the amount of silver can be increased to extend its effect towards intrinsically-resistant strains such as *P. aeruginosa*. Moreover, such reduced silver antibacterial activity has been observed mostly for alumina and zirconia coatings, whereas for silica the effect was preserved. This behavior can be explained by the ability of silica coatings per-se to enhance the effect of reactive oxygen species generated by silver ions as previously reported by Ortelli et al. (2018) who observed a photocatalytic production of reactive oxygen species by introducing silica as a bioactive coating for titanium nanoparticles.

24

Washing test

A washing test was performed on SiO2-Ag3, Al2O3-Ag3 and ZrO2-Ag3 to evaluate the resistance of the matrices to laundering. The results of the EDS analysis are reported in Fig. 8 9, for after 1, 5 and 10 washing cycles, together with photographs of the samples, to compare the data with the original samples. In general, the cotton appeared dark after the coating deposition, because of the absorption effect of the silver nanoclusters, but the color of the coating tended to disappear after the washing cycles, as a result of the dissolution of the coating in water.

The evident change in color of the silica-based coatings (Fig. 8 9a) suggested a poor resistance of the matrix when in contact with water. The EDS analysis, performed on samples after the washing test, confirmed that the amount of Si was halved after the first wash, and it was almost reduced to zero after 10 washes; subsequently, the Ag/Ag+Si ratio increased to 0.78, as the silica matrix dissolved in water faster than the silver one. Similar results were obtained for the Al2O3-Ag3 samples (Fig. 8 9b). The alumina content was reduced by around 50% after the first wash, while the amount of Ag decreased slowly. Instead, the change in color of the zirconia matrix samples was less visible (Fig. 8 9c). The reduction in the amount of Zr after 10 washing cycles amounted to only 30%, and a similar rate was observed for silver, as confirmed by the constant Ag/Ag+Zr atomic ratio after several washing cycles. The zirconia composite coatings dissolved slowly in water and exhibited a better resistance when in contact with water than the other matrices. This aspect was also in agreement with the results obtained from leaching test (Fig 7), where ZrO2-Ag3 coating released the lowest amount of silver (about 0.25 ppm) in water after 14 days vs 0.4 ppm for Al2O3-Ag3 and 0.3 ppm for SiO2-Ag3.
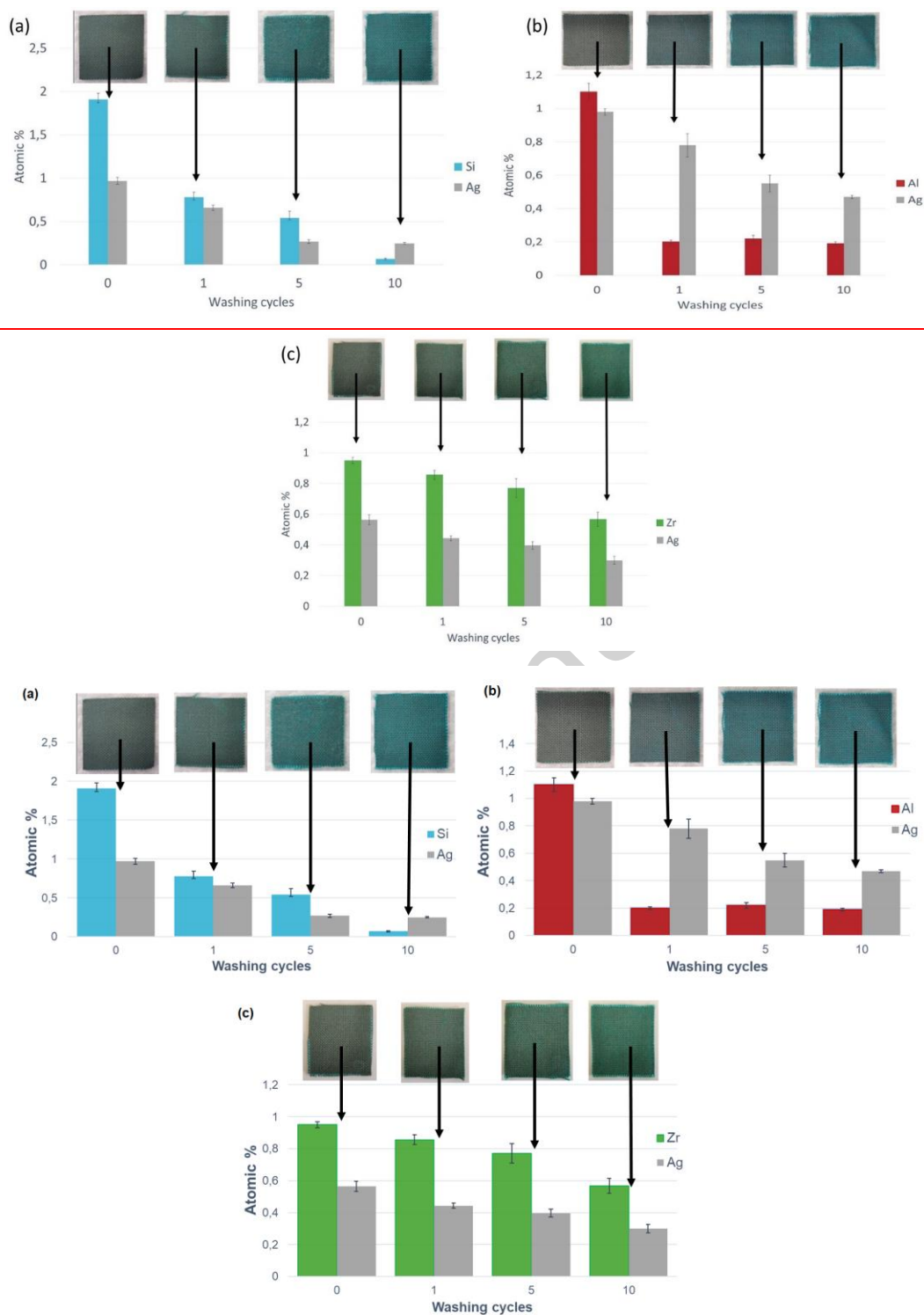
25

Fig. 8 9 The atomic percentage of coatings after 0, 1, 5 and 10 washing cycles (a) SiO2-Ag3, (b) Al2O3-Ag3, and (c) ZrO2-Ag3

The antibacterial properties of the same samples were verified before and after the washing test. Fig. 9–10 shows photographs of the inhibition halo test of the uncoated cotton (a) and before (b, d, f) and after 10 washing cycles (c, e, g) of cotton coated with the three silica, alumina and zirconia matrix composite

26

coatings with silver nanoclusters (only Ag3W). In agreement with the antibacterial tests described in the previous paragraph, all three coatings but not the uncoated cotton as control, demonstrated antibacterial properties, even toward *S. epidermis.* In fact, a bacteria-free halo formed around the samples before the washing test (Fig. 9-10 b,d,f), not visible around the uncoated cotton (Fig. 10a). The halo remained almost unchanged after the washing process (Fig. 9-10c, e, g), thereby showing that the antibacterial effect had been maintained, even though the amount of Ag detected by means of EDS had decreased.
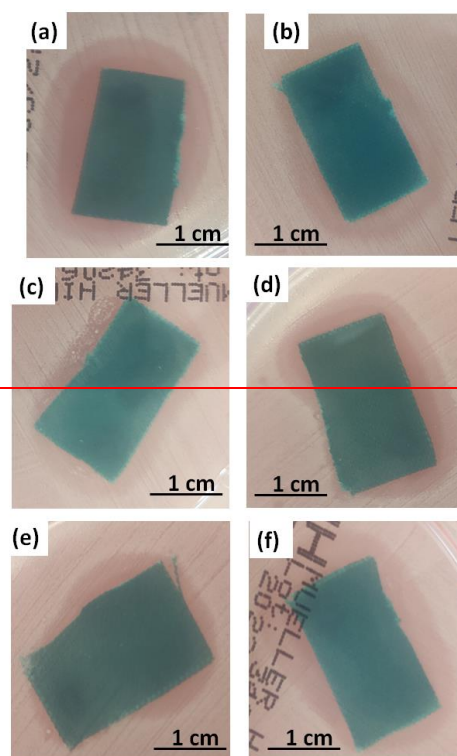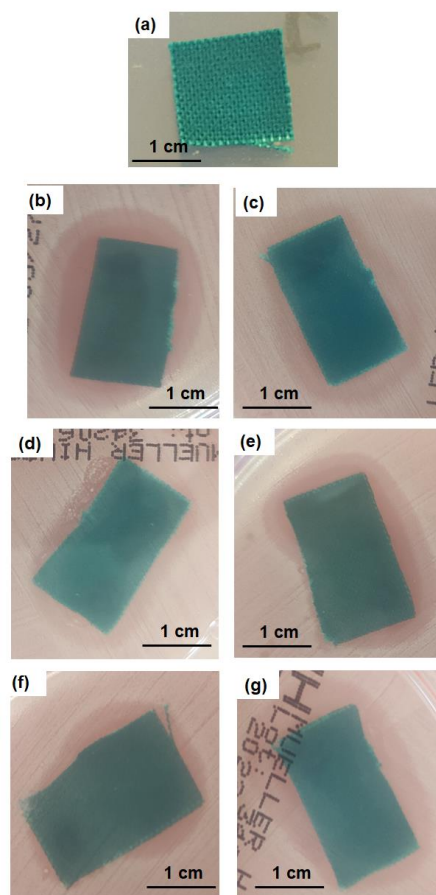
Fig. 9 10 Inhibition halo test of uncoated cotton (a) and coated cotton before washing (on the left) and after 10 cycles of washing (on the right): (b, c) SiO2-Ag3, (d, e) Al2O3-Ag3, and (f, g) ZrO2-Ag3.

Cytocompatibility evaluation

Considering that the here developed coating for textiles are not intended to be implanted neither to stay in contact with open-wound tissues, the ISO 10993 standard guidelines have been firstly followed to evaluate the potential release of toxic compounds from the coated materials. Accordingly, media have been pre-conditioned in direct contact with uncoated cotton (cnt) and coated cotton for 7 days in physiological conditions (37°C, pH 7,4) in order to promote the release of the potentially toxic compounds; afterwards, supernatants were collected and used to cultivated human fibroblasts (HGF) and human keratinocytes (HACAT). Such cells lines were selected as representative for the dermis and epidermidis, respectively, because they represent the first tissues in direct contact with the textiles and so they can suffer from the cytotoxic effect due to the adsorption of released toxic elements. Results of the indirect assay are reported in Figure 11 and Figure 12 for HGF and HACAT, respectively.

28

The metabolic activity of both HGF (Fig. 11a) and HACAT (Fig. 12a) was not significantly reduced by the presence of the released compounds as no statistically significant differences were detected between uncoated cotton as control (cnt) and coated substrates (p>0.05.) As a consequence, when the results from the coated cotton samples were normalized towards the control that was assumed being 100% viability, HGF reported values >93% for HGF (Fig. 11b) and >98% for HACAT (Fig. 12b). Interestingly, the effect was found to be not dose-dependent since no significant differences were detected between the lowest Ag-concentration groups (Ag3) and the highest ones (Ag5) thus suggesting that both concentrations belong to a cytocompatible ratio. Finally, as a visual confirmation of the metabolic activity results, when fluorescent dyes were applied to stain cells cultivated with pre-conditioned media, the cells' density was comparable between uncoated and coated cotton as a comparable number of nuclei was detected by the nuclear DAPI dye (Fig. 11c and 12c, stained in blue). Similarly, the phalloidin staining confirmed that cells properly adhered and spread by reporting a physiological elongated-shaped morphology for HGF (Fig. 11c, stained in green) and stellate-like for HACAT (Fig 12c, stained in green) that typically arrange in the observed clusters.
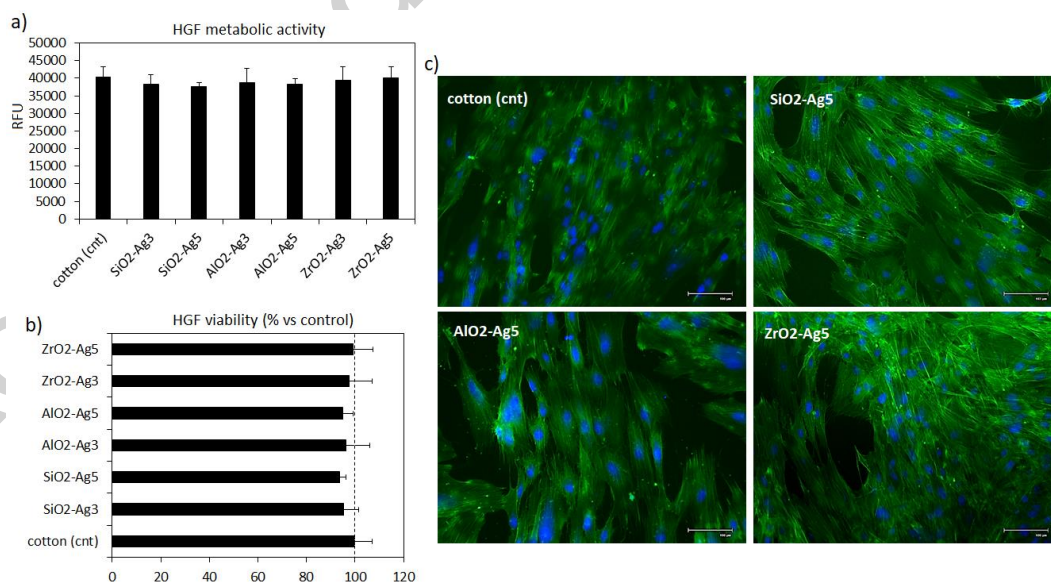

Fig. 11 Human fibroblasts (HGF) indirect cytocompatibility evaluation. (a) Cells' metabolic activity was not decreased by the release of toxic compounds by coated textiles as results were not significant in comparison to uncoated cotton as control (cnt) (p>0.05); (b) as a confirmation cells' viability was >95% if normalized to the cotton control considered as 100%. (c) Fluorescence

imaging of cells reported a comparable density and morphology between control (cotton) and coated samples. Images bar scale = 100 μm.

Fig. 12 Human keratinocytes (HACAT) indirect cytocompatibility evaluation. (a) Cells' metabolic activity was not decreased by the release of toxic compounds by coated textiles as results were not significant in comparison to uncoated cotton as controls (cnt) (p>0.05); (b) as a confirmation cells' viability was >98% if normalized to the cotton control considered as 100%. (c) Fluorescence imaging of cells reported a comparable density and morphology between control (cotton) and coated samples. Images bar scale = 100 μm.
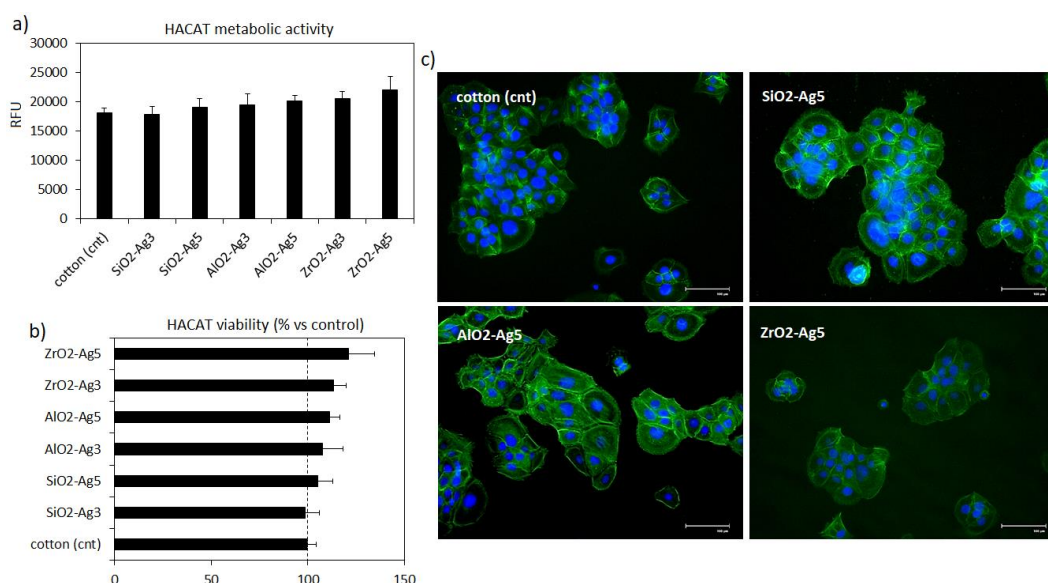
Then, although the primary focus of these textiles is not on implantation or direct wound contact, a direct assay was performed in order to exclude any other toxic effect due to the direct contact of tissues with the textiles, by seeding cells directly onto the surface of the uncoated and coated cotton. By this way, it was possible to observe the ability of cells to adapt and survive to the coated surfaces, assuming a prolonged direct contact. Accordingly, the cells were cultivated for 48hs onto the surface of the textiles and then their metabolic activity was checked by alamar blue whereas their adhesion and morphology were visually assessed by SEM. The results of the direct cytocompatibility evaluation towards human fibroblasts and keratinocytes are summarized in Figure 13 and Figure 14, respectively. In general, results were comparable with the previous indirect assay as no significant differences were detected for the HGF metabolic activity (Fig. 13a) and HACAT cells as well (Fig. 14a) by comparing cells cultivated onto uncoated cotton as control and all the coated textile materials (p>0.05). A slight decrease of cells'

30

viability was observed in comparison to the indirect assay because HGF reported values >79% (Fig. 13b) and HACAT >87%, but such results were not statistically significant in comparison to the controls (p>0.05). As a visual confirmation, SEM images evinced the presence of cells with an elongated shape adhering within the interconnected cotton fibers of the textiles that were recognized being the seeded HGF (Fig. 13c, indicated by the red arrows). Similarly, it was possible to appreciate stellate-like cells aligning onto cotton fibers when HACAT cells were investigated (Fig. 14c, indicated by the red arrows), thus confirming that textiles are not toxic and they can stay in contact with tissues even for long times without providing side effects.

Fig. 13 Human fibroblasts (HGF) direct cytocompatibility evaluation. (a) Cells' metabolic activity was not decreased by the direct contact with the coated textiles and results were not significant in comparison to uncoated cotton as controls (p>0.05); (b) as a confirmation cells' viability was >80% if normalized to the cotton as control considered as 100%. (c) SEM imaging of cells reported a comparable cells' adaptation to the uncoated or coated fibers (indicated by the red arrows). SEM images bar scale = 10 μm.
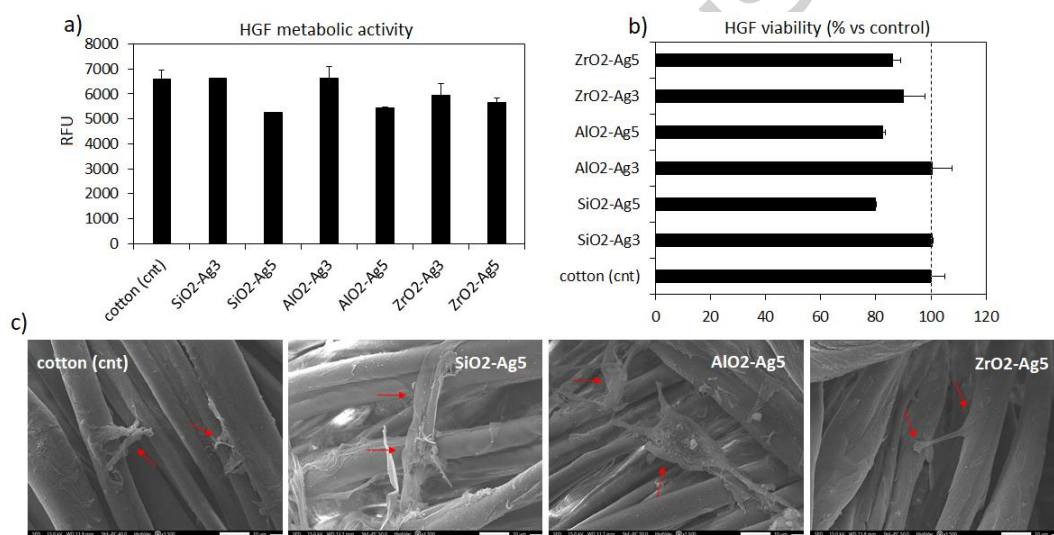
31

Fig. 14 Human keratinocytes (HACAT) direct cytocompatibility evaluation. (a) Cells' metabolic activity was not decreased by the direct contact with the coated textiles and results were not significant in comparison to uncoated cotton as control (p>0.05); (b) as a confirmation cells' viability was >89% if normalized to the cotton as control considered as 100%. (c) SEM imaging of cells reported a comparable cells' adaptation to the uncoated or coated fibers (indicated by the red arrows). SEM images bar scale = 10 μm.
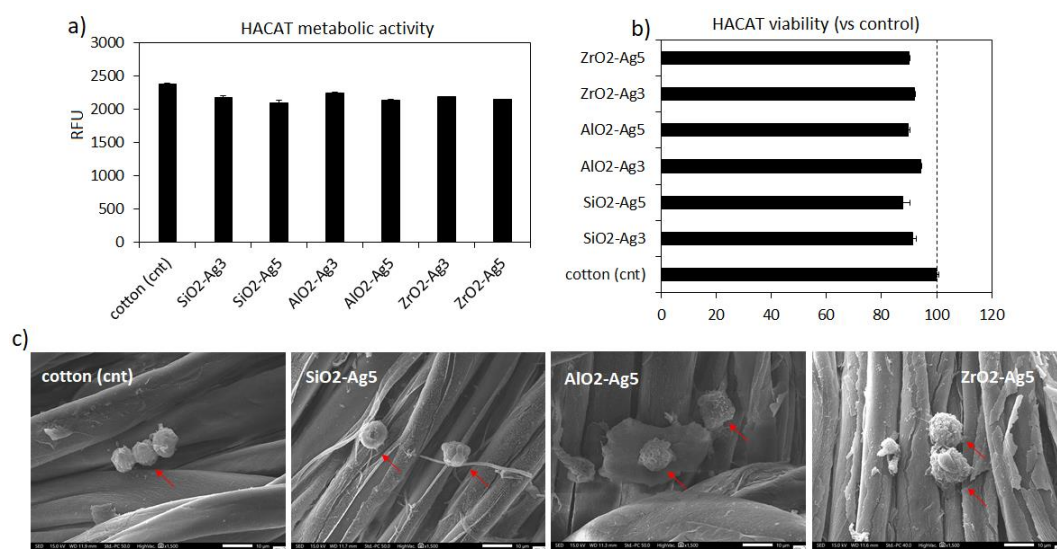
Conclusions

In conclusion, cotton textiles were uniformly coated with three composite coatings, with different compositions, via the co-sputtering method. The thin coatings were composed of silica, alumina or a zirconia matrix with embedded silver nanoclusters. Thanks to the modulation of the power on the target, it was possible to obtain coatings with an adequate amount of silver, and with a good compromise in terms of low ion release, antibacterial effect and washing resistance. All the coatings released silver ions into the water in the low 0.25-0.6 ppm range after 14 days, which is a value that is below the toxicity threshold. They demonstrated a significant antibacterial effect that could prevent contamination, even though a certain Ag dose-dependent effect was observed, thus suggesting the need to use a large amount of Ag (applying 5W of the power to the target instead of 3W) for some applications. The durability of the antibacterial properties was verified after ten washing cycles under conditions in which a washing machine process was simulated, and it was found that all the coatings had maintained their antibacterial effect, even though the amount of Ag detected by means of EDS had decreased. Finally, all the coatings were well-

32

tolerated by human cells representative for dermis and epidermidis, both if directly applied on the surface or after being in contact with pre-conditioned medium, thus excluding the release of toxic compounds when applied in contact with tissues.

33

Reference

AkbarShah M, Masood Pirzada B, Price G, Shibiru AL, Qurashi A (2022) Applications of nanotechnology in smart textile industry: A critical review. J Adv Res 38: 55-75. https://doi.org/10.1016/j.jare.2022.01.008

Allegranzi B, Gayet-Ageron A, Damani N et al (2013) Global implementation of WHO's multimodal strategy for improvement of hand hygiene: a quasi-experimental study. Lancet Infect Dis13:843-51. https://doi.org/10.1016/S1473-3099(13)70163-4

Angelina JTT, Ganesan S, Panicker TMR, Narayani R, Korath MP, Jagadeesan K (2017) Pulsed laser deposition of silver nanoparticles on prosthetic heart valve material to prevent bacterial infection. Mater Technol 32:148–155. https://doi.org/10.1080/10667857.2016.1160503

Deshmukh SP, Patil SM, Mullani SB, Delekar SD (2019) Silver nanoparticles as an effective disinfectant: A review. Mater Sci Eng C 97:954–965. https://doi.org/10.1016/j.msec.2018.12.102

Balagna C, Irfan M, Perero S, Miola M, Maina G, Santella D, Simone A (2017) Characterization of antibacterial silver nanocluster/silica composite coating on high performance Kevlar® textile. Surf Coat Technol 321:438–447. https://doi.org/10.1016/j.surfcoat.2017.05.009

Balagna C, Irfan M, Perero S, et al (2019) Antibacterial nanostructured composite coating on high performance Vectran™ fabric for aerospace structures. Surf Coat Technol 373:47–55. https://doi.org/10.1016/J.SURFCOAT.2019.05.076

Balagna C, Perero S, Bosco F, Mollea C, Irfan M, Ferraris M (2020) Antipathogen nanostructured coating for air filters. Appl Surf Sci 508:145283. https://doi.org/10.1016/j.apsusc.2020.145283

Balagna C, Perero S, Percivalle E, Nepita EV, Ferraris M (2020) Virucidal effect against coronavirus SARS-CoV-2 of a silver nanocluster/silica composite sputtered coating. Open Ceram 1:100006. https://doi.org/10.1016/j.oceram.2020.100006

Balagna C, Francese R, Perero S, Lembo D, Ferraris M (2021) Nanostructured composite coating endowed with antiviral activity against human respiratory viruses deposited on fibre-based air filters. Surf Coat Technol 409:126873. https://doi.org/10.1016/j.surfcoat.2021.126873

Bruna T, Maldonado-Bravo F, Jara P, Caro N (2021) Silver nanoparticles and their antibacterial applications. Int J Mol Sci 22: 7202. https://doi.org/10.3390/ijms22137202

Cochis A, Barberi J, Ferraris S, et al (2020) Competitive surface colonization of antibacterial and bioactive materials doped with strontium and/or silver ions. Nanomaterials 10: 120. https://doi.org/10.3390/nano10010120

Deshmukh SP, Patil SM, Mullani SB, Delekar SD (2019) Silver nanoparticles as an effective disinfectant: A review. Mater Sci Eng C 97:954–965. https://doi.org/10.1016/j.msec.2018.12.102

Ferraris M, Perero S, Miola M et al. (2010) Chemical, mechanical, and antibacterial properties of silver nanocluster–silica composite coatings obtained by sputtering. Adv Eng Mat 12: B276–B282. https://doi.org/10.1002/adem.200980076

Ferraris M, Perero S, Miola M, Ferraris S, Verné E, Morgiel J (2010) Silver nanocluster–silica composite coatings with antibacterial properties. Mater Chem Phys 120:123–126. https://doi.org/10.1016/j.matchemphys.2009.10.034

Ferraris M, Balagna C, Perero S (2019) Method for the Application of an Antiviral Coating to a Substrate and Relative Coating WO2019/082001

Fijan S, Pahor D, Turk SS (2017) Survival of Enterococcus faecium, Staphylococcus aureus and Pseudomonas aeruginosa on cotton. Text Res J 87:1711-1721. https://doi.org/10.1177/0040517516658514

Gao Y, Cranston R (2008) Recent Advances in Antimicrobial Treatments of Textiles. Text Res J 78:60–72. https://doi.org/10.1177/0040517507082332

Gottardi G, Laidani N, Victor M, Bartali R, Anderle M (2008) Effects of oxygen concentration in the Ar/O 2 plasma on the bulk structure and surface properties of RF reactively sputtered zirconia thin films. Surf Coat Technol 202: 2332–2337. https://doi.org/10.1016/j.surfcoat.2007.08.052.

Granados A, Pleixats R, Vallribera A (2021) Recent Advances on Antimicrobial and Anti-Inflammatory Cotton Fabrics Containing Nanostructures. Molecules 26:3008. https://doi.org/10.3390/molecules26103008

Hadrup N, Sharma AK, Loeschner K (2018) Toxicity of silver ions, metallic silver, and silver nanoparticle materials after in vivo dermal and mucosal surface exposure: A review. Regul Toxicol Pharmacol 98:257–267. https://doi.org/10.1016/j.yrtph.2018.08.007

Heudorf U, Gasteyer S, Müller M, et al (2016) Handling of laundry in nursing homes in Frankfurt am Main, Germany, 2016–laundry and professional clothing as potential pathways of bacterial transfer." GMS Hyg Infec Control 12: Doc20. https://doi.org/10.3205/dgkh000305

35

Ibrahim A, Laquerre J-É, Forcier P, Deregnaucourt V, Decaens J, Vermeersch O (2021) Antimicrobial agents for textiles: types, mechanisms and analysis standards. In: Kumar B (ed) Textiles for Functional Applications, IntechOpen, London. https://doi.org/10.5772/intechopen.98397.

Irfan M, Perero S, Miola M, et al (2017) Antimicrobial functionalization of cotton fabric with silver nanoclusters/silica composite coating via RF co-sputtering technique. Cellulose 24: 2331–2345. https://doi.org/10.1007/s10570-017-1232-y

Jain A, Kongkham B, Puttaswamy H, Butola BS, Malik HK, Malik A (2022) Development of Wash-Durable Antimicrobial Cotton Fabrics by In Situ Green Synthesis of Silver Nanoparticles and Investigation of Their Antimicrobial Efficacy against Drug-Resistant Bacteria. Antibiotics 11:864. https://doi.org/10.3390/ antibiotics11070864

Jamuna-Thevi K, Bakar SA, Ibrahim S, Shahab N,Toffa MRM, et al (2011) Quantification of silver ion release, in vitro cytotoxicity and antibacterial properties of nanostuctured ag doped TiO_2 coatings on stainless steel deposited by rf magnetron sputtering. Vacuum 86:235–241. https://doi.org/10.1016/j.vacuum.2011.06.011

Jayaseelan S, Ramaswamy D, Dharmaraj S. (2014) Pyocyanin: production, applications, challenges and new insights. World J Microbiol Biotechnol. 30:1159-68. https://doi.org/10.1007/s11274-013-1552-5

Jazbec K, Šala M, Mozetič M, Vesel A, Gorjanc M (2015) Functionalization of cellulose fibres with oxygen plasma and ZnO Nanoparticles for Achieving UV Protective Properties. J Nanomater 2015:346739. https://doi.org/10.1155/2015/346739.

Kowalczyk D, Brzeziński S, Kamińska I (2018) Multifunctional nanocoating finishing of polyester/cotton woven fabric by the sol-gel method. Text Res J 88:946–956. https://doi.org/10.1177/0040517517693979.

Krylova GV, Gnatyuk YI, Smirnova NP, et al (2009) Ag nanoparticles deposited onto silica, titania, and zirconia mesoporous films synthesized by sol–gel template method. J Sol-Gel Sci Technol 50:216–228. https://doi.org/10.1007/s10971-009-1954-x

Liu C, Liao D, Ma F, Huang Z, Liu J, Mohamed IMA (2021) Enhanced conductivity and antibacterial behavior of cotton via the electroless deposition of silver. Molecules 26:4731. https://doi.org/10.3390/molecules26164731.

Mishra A, Butola BS (2017) Deposition of Ag doped TiO2 on cotton fabric for wash durable UV protective and antibacterial properties at very low silver concentration. Cellulose 24:3555–3571 https://doi.org/10.1007/s10570-017-1352-4

Muller M, Merrett ND (2014) Pyocyanin production by Pseudomonas aeruginosa confers resistance to ionic silver. Antimicrob Agents Chemother 58:5492-9. https://doi.org/10.1128/AAC.03069-14

NCCLS M2-A9 (2003) Performance Standards for Antimicrobial Disk Susceptibility Tests, Approved Standard, 9th Edn, NCCLS, Villanova, PA, USA 2003

Ortelli S, Costa AL, Matteucci P, Miller MR, Blosi M, Gardini D, Tofail SAM, Tran L, Tonelli D, Poland CA (2018) Silica modification of titania nanoparticles enhances photocatalytic production of reactive oxygen species without increasing toxicity potential in vitro. RSC Adv 8:40369-40377. https://doi.org/10.1039/C8RA07374K

Owen L, Laird K (2020) The role of textiles as fomites in the healthcare environment: a review of the infection control risk. PeerJ 8:e9790. https://doi.org/10.7717/peerj.9790

Pal S, Tak YK, Song JM (2007) Does the antibacterial activity of silver nanoparticles depend on the shape of the nanoparticle? A study of the gram-negative bacterium Escherichia coli. Appl Env Microbiol 73:1712–1720. https://doi.org/10.1128/AEM.02218-06

Park SH, Kim SH, Park SJ, et al (2016) Direct incorporation of silver nanoparticles onto thin-film composite membranes via arc plasma deposition for enhanced antibacterial and permeation performance. J Membr Sci 513:226–235. https://doi.org/10.1016/j.memsci.2016.04.013

Periolatto M, Ferrero F, Vineis C, Varesano A, Gozzelino G (2017) Novel antimicrobial agents and processes for textile applications. In Kumavath RN (ed) Antibacterial Agents, IntechOpen, London https://doi.org/10.5772/intechopen.68423

Radetić M (2013) Functionalization of textile materials with silver nanoparticles. J Mater Sci 48:95–107. https://doi.org/10.1007/s10853-012-6677-7

Rai M, Yadav A, Gade A (2009) Silver nanoparticles as a new generation of antimicrobials. Biotechnol Adv 27:76–83. https://doi.org/10.1016/j.biotechadv.2008.09.002

Raza ZA, Rehman A, Mohsin M, Bajwa SZ, Anwar F, Naeem A, Ahmad N (2015) Development of antibacterial cellulosic fabric via clean impregnation of silver nanoparticles. J Clean Prod 101:377–386. https://doi.org/10.1016/j.jclepro.2015.03.091

Rehan M, Mashaly H, Mowafi S, El-Kheir A, Emam H (2015) Multi-functional textile design using in-situ Ag NPs incorporation into natural fabric matrix. Dyes Pigments118:9-17 https://doi.org/10.1016/j.dyepig.2015.02.021.

Riley K, Williams J, Owen L, Shen J, Davies A, Laird K (2017) The effect of low-temperature laundering and detergents on the survival of Escherichia coli and Staphylococcus aureus on textiles used in healthcare uniforms. J Appl Microbiol 123: 280-286. https://doi.org/10.1111/jam.13485

Rivera LR, Cochis A, Biser S, Canciani E, Ferrraris S, Rimondini L, Boccaccini A (2021) Antibacterial, pro-angiogenic and pro-osteointegrative zein-bioactive glass/copper based coatings for implantable stainless steel aimed at bone healing. Bioact Mater 6:1479-1490. https://doi.org/10.1016/j.bioactmat.2020.11.001

Samuel E, Lee JG, Joshi B, et al (2017) Supersonic cold spraying of titania nanoparticles on reduced graphene oxide for lithium ion battery anodes J Alloy Compd 715:161–169. https://doi.org/10.1016/j.jallcom.2017.04.308.

Shaban M, Abdallah S, Khalek AA (2016) Characterization and photocatalytic properties of cotton fibers modified with ZnO nanoparticles using sol–gel spin coating technique. Beni-Suef Univ J Basic Appl Sci 5:277–283. https://doi.org/10.1016/j.bjbas.2016.08.003

Shahzad N, Chen F, Khan M (2016) Photovoltaic characteristics of titania photoanodes modified with silver nanoparticles by pulsed laser deposition. Mater Lett 163:266–269. https://doi.org/10.1016/j.matlet.2015.10.096.

Sharifikolouei E, Najmi Z, Cochis A, Scalia AC, Aliabadi M, Perero S, Rimondini L (2021) Generation of cytocompatible superhydrophobic Zr–Cu–Ag metallic glass coatings with antifouling properties for medical textiles. Mater Today Bio 12:100148. https://doi.org/10.1016/j.mtbio.2021.100148

Soliwoda K, Rosowski M, Tomaszewska E, Tkacz-Szczesna B, Celichowski G, Grobelny J (2015) Electrospray deposition of gold nanoparticles from aqueous colloids on solid substrates. Colloid Surf A: Physicochem Eng Asp 486:211–217. https://doi.org/10.1016/j.colsurfa.2015.09.035.

Souza TAJ, Lilian Rodrigues Rosa Souzac LRR, Franchia LP (2019) Silver nanoparticles: An integrated view of green synthesis methods, transformation in the environment, and toxicity. Ecotoxicol Environ Saf 171:691–700. https://doi.org/10.1016/j.ecoenv.2018.12.095

Stefanov P, Stoychev D, Stoycheva M, Ikonomov J, Marinova T (2000) XPS and SEM characterization of zirconia thin films prepared by electrochemical deposition. Surf Interface Anal 30:628–631. https://doi.org/10.1002/1096-9918(200008)30:1<628::AID-SIA800>3.0.CO;2-7

Tomšič B, Simončič B, Orelet B, al (2008) Sol-Gel coating of cellulose fibres with antimicrobial and repellent properties. J Sol-Gel SciTechnol 47:44–57. https://doi.org/10.1007/s10971-008-1732-1

Volkov IL, Smirnova, Makarova AA et al. (2017) DNA with Ionic, Atomic, and Clustered Silver: An XPS Study. J Phys Chem B 121:2400–2406. https://doi.org/10.1021/acs.jpcb.6b11218.

Weber RL, Khan PD, Fader RC, Weber RA (2012) Prospective study on the effect of shirt sleeves and ties on the transmission of bacteria to patients. J Hosp Infect 80: 252-254. https://doi.org/10.1016/j.jhin.2011.12.012

Windler L, Height M, Nowack B (2013) Comparative evaluation of antimicrobials for textile applications. Environ Int 53:62–73. https://doi.org/10.1016/j.envint.2012.12.010.

Zuzjaková Š, Zeman P, Kos Š (2013) Non-isothermal kinetics of phase transformations in magnetron sputtered alumina films with metastable structure Thermochim Acta 572:85–93. https://doi.org/10.1016/j.tca.2013.09.019

Statements & Declarations

Funding

Competing Interests

The authors have no relevant financial or non-financial interests to disclose.

Author Contributions

Angelica Luceri, Sergio Perero, Monica Ferraris and Cristina Balagna contributed to the study conception. Material preparation, research and experimental data collection and analysis were performed by Angelica Luceri, Sergio Perero, Andrea Civra, Alessandro C. Scalia and Cristina Balagna. The research activity was supervised by Monica Ferraris, Cristina Balagna, Andrea Civra and Lia Rimondini. The first draft of the manuscript was written by Angelica Luceri and Cristina Balagna with the Andrea Civra's contribution. All authors commented on previous versions of the manuscript. All authors read and approved the final manuscript.

Ethics approval and consent to participate

Not applicable

Consent for publication

Not applicable

Availability of data and materials

Data sharing is not applicable to this article as no datasets were generated or analysed during the current study

Figure captions

Fig. 1 XPS survey spectra of the (a) uncoated cotton, (b) silica-based coating (SiO2-Ag3), (c) alumina-based coating (Al2O3-Ag3), and (d) zirconia-based coating (ZrO2-Ag3).

Fig. 2 High resolution XPS spectra of carbon, oxygen, the metals of the matrix oxides (Si, Al and Zr) and silver: comparison among the cotton coated with the three coatings of silica or alumina or zirconia and silver nanoclusters (3W) and the uncoated cotton.

Fig. 3 XRD analysis of the coatings (a) SiO2-Ag, (b) Al2O3-Ag, and (c) ZrO2-Ag with the two different silver concentrations (Ag5, high amount, and Ag3, low amount), and comparison of the spectra with those obtained for the corresponding matrix (silica, alumina or zirconia, respectively). *(Samples deposited on soda-lime substrates)*

Fig. 4 Uv-Visible analysis of the (a) SiO2-Ag, (b) Al2O3-Ag, and (c) ZrO2-Ag coatings *(Samples deposited on soda-lime substrates)*

Fig. 5 FESEM images of the (a) uncoated cotton and cotton with coatings, (b) SiO2-Ag3, (c) SiO2-Ag5, (d) Al2O3-Ag3, (e) Al2O3-Ag5, (f) ZrO2-Ag3, and (g) ZrO2-Ag5. The red arrows indicate the presence of Ag nanoclusters on the coating surface.

Fig. 6 FESEM images in back scattered mode of cotton with coatings, (a) SiO2-Ag5, (b) Al2O3-Ag5 and (c) ZrO2-Ag5. The red arrows indicate the presence of Ag nanoclusters on the coating surface.

Fig. 6 7 Ions released from the silica, alumina and zirconia-based coatings with Ag at 3W and 5W *versus* time.

Fig. 7 8 Antibacterial evaluation: histograms of the number of viable CFUs of (a) *E. coli* and (b) *P. aeruginosa* contaminating the three composite coatings with the low and the high Ag contents. Uncoated cotton was used as a control (n.d. = colonies not detected; # = $p < 0.05$). (c) representative pictures of the living *P. aeruginosa* colonies after detachment from the composite coatings containing a large amount of silver (Ag5).

Fig. 8 9 The atomic percentage of coatings after 0, 1, 5 and 10 washing cycles (a) SiO2-Ag3, (b) Al2O3-Ag3, and (c) ZrO2-Ag3

Fig. 9 10 Inhibition halo test of uncoated cotton (a) and coated cotton before washing (on the left) and after 10 cycles of washing (on the right): (b, c) SiO2-Ag3, (d, e) Al2O3-Ag3, and (f, g) ZrO2-Ag3.

Fig. 11 Human fibroblasts (HGF) indirect cytocompatibility evaluation. (a) Cells' metabolic activity was not decreased by the release of toxic compounds by coated textiles as results were not significant in comparison to uncoated cotton as control (cnt) ($p > 0.05$); (b) as a confirmation cells' viability was >95% if normalized to the cotton control considered as 100%. (c) Fluorescence imaging of cells reported a comparable density and morphology between control (cotton) and coated samples. Images bar scale = 100 μm.

Fig. 12 Human keratinocytes (HACAT) indirect cytocompatibility evaluation. (a) Cells' metabolic activity was not decreased by the release of toxic compounds by coated textiles as results were not significant in comparison to uncoated cotton as controls (cnt) (p>0.05); (b) as a confirmation cells' viability was >98% if normalized to the cotton control considered as 100%. (c) Fluorescence imaging of cells reported a comparable density and morphology between control (cotton) and coated samples. Images bar scale = 100 μm

Fig. 13 Human fibroblasts (HGF) direct cytocompatibility evaluation. (a) Cells' metabolic activity was not decreased by the direct contact with the coated textiles and results were not significant in comparison to uncoated cotton as controls (p>0.05); (b) as a confirmation cells' viability was >80% if normalized to the cotton as control considered as 100%. (c) SEM imaging of cells reported a comparable cells' adaptation to the uncoated or coated fibers (indicated by the red arrows). SEM images bar scale = 10 μm.

Fig. 14 Human keratinocytes (HACAT) direct cytocompatibility evaluation. (a) Cells' metabolic activity was not decreased by the direct contact with the coated textiles and results were not significant in comparison to uncoated cotton as control (p>0.05); (b) as a confirmation cells' viability was >89% if normalized to the cotton as control considered as 100%. (c) SEM imaging of cells reported a comparable cells' adaptation to the uncoated or coated fibers (indicated by the red arrows). SEM images bar scale = 10 μm.

.

Table 1: The atomic percentages of the metallic element in the matrix (M) and Ag as a function of the power applied to the Ag target, and the relative ratio value

Power on Ag (W)	%at.	SiO$_2$	Al$_2$O$_3$	ZrO$_2$
	M	2.18 ± 0.02	1.10 ± 0.05	0.95 ± 0.02
3	Ag	1.11 ± 0.02	0.98 ± 0.02	0.56 ± 0.03
	Ag/M+Ag	0.34	0.47	0.37
	M	2.60 ± 0.07	1.51 ± 0.09	1.17 ± 0.03
5	Ag	2.81 ± 0.05	1.37 ± 0.05	1.14 ± 0.08
	Ag/M+Ag	0.52	0.48	0.49

43

Table 2: XPS analysis of the composition of the cotton surface in %at. and comparison of the data from the uncoated and coated cotton with the three composite coatings containing Ag at 3W.

	at.%					
	C1s	O1s	Si2p	Al2p	Zr3	Ag3d
Cotton	79	20	-	-	-	-
SiO2-Ag3	29	49	18	-	-	4
Al2O3-Ag3	44	36	-	15	-	5
ZrO2-Ag3	40	42	-	-	14	5

44